J Membrane Biol (2009) 228:125–140
DOI 10.1007/s00232-009-9165-5

ORIGINAL ARTICLES

Slc26a9—Anion Exchanger, Channel and Na^+ Transporter

Min-Hwang Chang · Consuelo Plata · Kambiz Zandi-Nejad · Aleksandra Sinđić · Caroline R. Sussman · Adriana Mercado · Vadjista Broumand · Viswanathan Raghuram · David B. Mount · Michael F. Romero

Received: 15 January 2009 / Accepted: 3 March 2009 / Published online: 14 April 2009

Abstract The SLC26 gene family encodes anion transporters with diverse functional attributes: (a) anion exchanger, (b) anion sensor, and (c) anion conductance (likely channel). We have cloned and studied Slc26a9, a paralogue expressed mostly in lung and stomach. Immunohistochemistry shows that Slc26a9 is present at apical and intracellular membranes of lung and stomach epithelia. Using expression in *Xenopus laevis* oocytes and ion-sensitive microelectrodes, we discovered that Slc26a9 has a novel function not found in any other Slc26 proteins: cation coupling. Intracellular pH and voltage measurements show that Slc26a9 is a $n\mathrm{Cl}^-$-HCO_3^- exchanger, suggesting roles in gastric HCl secretion or pulmonary HCO_3^- secretion; Na^+ electrodes and uptakes reveal that Slc26a9 has a cation dependence. Single-channel measurements indicate that Slc26a9 displays discrete open and closed states. These experiments show that Slc26a9 has three discrete physiological modes: $n\mathrm{Cl}^-$-HCO_3^- exchanger, Cl^- channel, and Na^+-anion cotransporter. Thus, the Slc26a9 transporter channel is uniquely suited for dynamic and tissue-specific physiology or regulation in epithelial tissues.

Keywords Intracellular pH · Cl^- · Na^+ · HCO_3^- · *Xenopus* oocyte expression · Epithelial localization

Min-Hwang Chang, Consuelo Plata, and Kambiz Zandi-Nejad have contributed equally to this work.

M.-H. Chang · C. Plata · A. Sinđić · C. R. Sussman · M. F. Romero
Physiology & Biophysics, Case Western Reserve University, Cleveland, OH 44106, USA

M.-H. Chang · A. Sinđić · C. R. Sussman · M. F. Romero (✉)
Department of Physiology & Biomedical Engineering, Mayo Clinic College of Medicine, 200 First Street SW, Rochester, MN 55905, USA
e-mail: romero.michael@mayo.edu

C. Plata
Instituto Nacional de Ciencias Médicas y Nutrición Salvador Zubirán, Mexico 14000, México

K. Zandi-Nejad · A. Mercado · V. Broumand · D. B. Mount
Renal Division, Brigham & Women's Hospital, Boston, MA 02115, USA

A. Sinđić
Physiology, School of Medicine, Croatian Institute for Brain Research, University of Zagreb, Zagreb, Croatia

V. Raghuram
NHLBI, NIH, Bethesda, MD 20892, USA

D. B. Mount
Renal Division, VA Boston Healthcare System, West Roxbury, MA 02132, USA

The Slc26 gene family encodes 10 transport proteins with diverse physiology. Slc26a1 (Sat-1) encodes a SO_4^{2-} transporter shown to exchange SO_4^{2-} for oxalate (Bissig et al. 1994) and possibly HCO_3^-. Other family members were identified by positional cloning of disease genes: diastrophic dysplasia (SLC26A2/DTDST) (Hastbacka et al. 1992), congenital chloride diarrhea (SLC26A3/DRA) (Hoglund et al. 1996; Schweinfest et al. 1993), and Pendred syndrome (SLC26A4/pendrin) (Everett et al. 1997). Slc26a5 (prestin) was identified as a "molecular motor" of cochlear outer hair cells (Zheng et al. 2000). SLC26A6 was identified as a candidate gene for the apical, exocrine pancreas, HCO_3^- transporter (Lohi et al. 2000) and the proximal tubule Cl^--formate exchanger (Knauf et al. 2001).

Many anions are transported by SLC26 proteins (Bissig et al. 1994; Karniski et al. 1998; Moseley et al. 1999; Mount

and Romero 2004; Satoh et al. 1998; Scott and Karniski 2000; Soleimani et al. 2001): SO_4^{2-}, Cl^-, I^-, formate$^-$, oxalate^{2-} (ox^{2-}), OH^-, and HCO_3^-. Functional characterization of Slc26 proteins has revealed distinctive patterns of anion specificity, cis inhibition, and transport modes. Mouse Slc26a6 transports most of the above substrates (Xie et al. 2002a). In contrast, Slc26a1 transports SO_4^{2-} and ox^{2-} but not Cl^- or formate (Bissig et al. 1994; Karniski et al. 1998; Satoh et al. 1998; Xie et al. 2002a). SLC26A4 transports only monovalent anions, and not divalent anions (Scott and Karniski 2000; Scott et al. 1999).

The physiological role(s) of individual SLC26 anion exchangers is a function of both substrate specificity and tissue expression. As noted, the diverse physiological impact of Slc26 proteins is illustrated by loss-of-function (disease) phenotypes. SLC26A3 is found in colonic epithelial brush border membranes (Haila et al. 2001; Moseley et al. 1999) and helps to mediate colonic, transepithelial salt transport. Its mutation results in severe congenital diarrhea (Hoglund et al. 1996). SLC26A2 mutations cause disordered skeletal development by impairing SO_4^{2-} uptake of chondrocytes and resulting in decreased extracellular matrix sulfation (Hastbacka et al. 1996). This sulfation loss decreases responsiveness to matrix-dependent developmental cues, e.g., FGF.

Novel family members were initially noticed in databases of mammalian expressed sequence tags (ESTs) (Everett and Green 1999) and some initial characterization was reported (Lohi et al. 2002). Slc26a7 was initially reported to function as a Cl^--HCO_3^- exchanger (Petrovic et al. 2003) and, more recently, as an anion conductance (Kim et al. 2005). Slc26a9 was reported as a Cl^--HCO_3^- exchanger specific to gastric surface epithelia (Xu et al. 2005), while recent work portrays Slc26a9 as an anion conductance with minimal HCO_3^- transport (Dorwart et al. 2007). Notably, large cellular currents imply "channel activity," but such currents are not definitive evidence of channel function.

We cloned several of these novel Slc26 members (Xie et al. 2002b) and reported the initial detailed characterization of Slc26a6 as a novel electrogenic Cl^--$nHCO_3^-$ exchanger (Xie et al. 2002a). The present extensive analysis of Slc26a9 reveals that it has physiological activities *not* found together in any other Slc26 proteins: nCl^--HCO_3^- exchanger, Na^+/anion cotransporter, and anion channel. Importantly, we provide single-channel data and other experiments illustrating a Na^+-coupled transport mode. Slc26a9 is the first, and perhaps only, Slc26 member to show Na^+ (cation) coupling. We hypothesize that these diverse activities allow Slc26a9 to fulfill a wide variety of physiological roles in the lung and stomach and likely allow quick, dynamic physiological regulation in these tissues.

Methods

Animal Health and Welfare

Mice and Xenopus were housed and cared for in accordance and approval of the Institutional Care and Use Committees of Case Western Reserve University (mice and Xenopus), the Mayo Clinic (Xenopus), VA Boston Healthcare System, Brigham & Womens Hospital, and Instituto Nacional de Ciencias Médicas y la Nutrición Salvador Zubirán (Xenopus).

Cloning of SLC26A9 and Slc26a9

Human SLC26A9 exons were identified in BAC clone sequences (RP11-196022, RP11-370I5). 3′ SLC26A9 genomic sequences were used to search for human 3′-UTR ESTs. The identified IMAGE clone 2915384 was obtained and sequenced (bp 2502–4526 of the final cDNA). The open reading frame was then cloned by RT-PCR of human lung with Takara LaPCR polymerase with specific primers (Table 1). PCR fragments were subcloned into pCR2.1 (Invitrogen) and sequenced. A 500,000-bp contig containing the entire mouse Slc26a9 gene was identified by a *blastn* search of the Celera mouse genomic database with human SLC26A9 (*AF314958*). The Slc26a9 cDNA (3049 bp; *AY034145*) was amplified by RT-PCR from mouse lung with a mouse primers (Table 1) and subcloned into the *Xenopus laevis* expression vector pGEMHE.

Localization of Slc26a9 mRNA

Northern Analysis

RNA was extracted from mice using guanidine isothiocyanate and CsCl. Total RNA (10 µg/lane) was size-fractionated by electrophoresis (5% formaldehyde, 1% agarose), transferred to a nylon membrane (Stratagene), and probed with ^{32}P-labeled randomly-primed (DecaPrime; Ambion) gene-specific probes for Slc26a9 and full-length GAPDH. The Slc26a9 probe was generated by PCR (bp 2203–2810), as were the probes for human SLC26A9 (bp 291–822) and SLC26A6 (bp 2090–2587). Hybridization was overnight at 42°C (4 × SSCP/40% formamide/4 × Denhart's solution/0.5% SDS/200 µg salmon sperm DNA), and membranes were washed twice for 10 min at room temperature in 2 × SSCP/0.1% SDS and twice for 1 h at 65°C in 0.1 × SSCP/0.1% SDS.

RT-PCR

Total RNA (200 ng/reaction) from mouse tissues was reverse transcribed using oligo(dT) priming. PCR

Table 1 PCR primers used

Primer name	Primer sequence	Use
Human SLC26A9		
Forward	5′-TAgACAgAgCCgCATACTCCCTTACCCTCTTC-3′	Cloning SLC26A9
Reverse	5′-gATgTgCTTgCTgACAgCAgTggTggTTTgg-3′	Cloning SLC26A9
Mouse Slc26a9		
Forward	5′-CAAAgCTTgTCAATgTCCCAgACATgAACCAgC	Cloning mSlc26a9
Reverse	5′-CCACTgTCCACACTAgAgTCTgAAgTgCTggACAgC	Cloning mSlc26a9
Slc26a9		
Forward	5′-GCTGAGGCTCACATATCCTAC-3′	RT-PCR
Reverse	5′-AGAGGACTGCATCGTGGATG-3′	RT-PCR
GAPDH		
Forward	5′-TCACCATCTTCCAGGAGCG-3′	RT-PCR
Reverse	5′-CTGCTTCACCACCTTCTTGA-3′	RT-PCR

amplification was performed as described (Mount et al. 1999), using Taq-2000 polymerase (Stratagene). The Slc26a9 primers (Table 1) amplified a 354-bp band. RT-PCR with a GAPDH-specific primer pair (Table 1) amplified a 571-bp band.

Protein Localization

Slc26a9 Antibodies

To localize mSlc26a9, we generated two rabbit peptide antibodies against the C-terminus: "CQEL" (C-QELQQDFESAPSTDPNN) and "aCKQ" (acetyl-C-KQKYLRKQEKRTAIPTQQRK) (Quality Control Biochemicals, Hopkinton, MA). aCKQ had superior reactivity and was used for all experiments reported (now referred to as Slc26a9 antibody). We verified Slc26a9 antibody specificity by Western analysis of oocytes expressing Slc26 protein, as previously performed for other transporters (Schmitt et al. 1999; Sciortino et al. 2001). The Slc26a9 antibody recognized the appropriate-sized protein in Slc26a9 oocytes but not water-injected controls or cells expressing other SLC26 transporters (see Fig. 2A).

Immunohistochemistry

Mice were perfusion-fixed with PBS followed by 4% paraformaldehyde-lysine-periodate (PLP) (Schmitt et al. 1999). Tissues were dissected and fixed for several hours in PLP, followed by overnight 30% sucrose in PBS at 4°C (Sciortino et al. 2001). OCT (cryomedium)-embedded tissue was cryosectioned at 10 μm. Immunostaining was performed using a 1:100 dilution of the primary Slc26a9 antibody and a Cy3 secondary antibody. Epifluorescent images were captured using a Zeiss AxioVert 25 microscope (Dinour et al. 2004; Sciortino et al. 2001).

Oocyte Experiments

Female *X. laevis* were purchased from Xenopus Express (Beverly Hills, FL). Slc26 clones were subcloned into the pGEMHE *Xenopus* expression vector (Liman et al. 1992). Oocytes were collagenase-dissociated (Romero et al. 1998). Capped cRNA was synthesized using the T7 mMessage mMachine kit (Ambion, Austin, TX). Oocytes were injected with 50 nL cRNA (0.5 μg/μL, 25 ng/oocyte) or water and incubated at 16°C in OR_3 medium, unless otherwise indicated. Oocytes were studied 3–10 days after injection.

Uptake Experiments

$^{36}Cl^-$ and $^{22}Na^+$ uptakes were performed as previously (Plata et al. 2007; Xie et al. 2002a). Briefly, oocytes were preincubated for 20 min in 0-Cl^- ($0Cl^-$) and 0-Na^+ ($0Na^+$) uptake medium (mM: 100 NMDG-gluconate, 2 K-gluconate, 1 Ca-gluconate, 1 Mg-gluconate, 10 HEPES-Tris, pH 7.5). Oocytes were then incubated for 60 min with isotope. Cells were washed 3 × in uptake buffer with 5 mM cold uptake buffer. Oocytes were individually dissolved in 10% SDS and tracer activity was determined by scintillation counting. Cl^- uptake was performed using the same $0Cl^-$ uptake solution (8.3 mM $^{36}Cl^-$). For Na^+ experiments, we added 100 mM Na^+ to replace 100 mM NMDG and included furosemide (100 μM) to inhibit the oocyte Na^+-K^+-$2Cl^-$ cotransporter. The uptake experiments included 12–18 oocytes in each experimental group (mean ± SE). Statistical significance was $p < 0.05$ using a two-tailed Student's *t*-test.

Electrophysiology

All solutions were either ND96 (96 mM NaCl, 2 mM KCl, 1.8 mM $CaCl_2$, 1 mM $MgCl_2$, 5 mM HEPES, pH 7.5) or iso-osmotic ion replacements (Sciortino and Romero

1999). The Na^+ replacement was NMDG, and the Cl^- replacement was gluconate. For HCO_3^- solutions, we used 5% CO_2/33 mM HCO_3^- (pH 7.5).

Two-Electrode Voltage Clamp

For these experiments, oocytes were injected with 0.5 ng cRNA and membrane currents were recorded with an OC-725C voltage clamp (Warner Instruments, Hamden, CT), filtered at 2–5 kHz, and digitized at 10 kHz. I–V protocols consisted of 40-ms steps from V_h (−60 mV) to −160 mV and +60 mV in 20-mV steps (Dinour et al. 2004; Sciortino and Romero 1999).

Ion-Selective Microelectrodes

Ion-selective microelectrodes were used to monitor pH_i, Cl^- ($[Cl^-]_i$) and intracellular Na^+ activity ($[Na^+]_i$) of oocytes (Romero et al. 1998, 2000; Sciortino and Romero 1999). Intracellular pH, Cl^-, and Na^+ microelectrodes had slopes of at least −54 mV/pH unit or decade, respectively.

Patch-Clamp and Single-Channel Analysis

Most patch-clamp recordings were performed in excised inside-out patches of CHO cells (similar results were obtained with Slc26a9 oocytes or transfected HEK cells). Patch pipettes were 10–20 MΩ; membrane seals were >10 GΩ. The bath and pipette solutions contained (mM) 138 NMDG-Cl, 2 $MgCl_2$, and 10 HEPES (pH 7.5). All experiments were performed at room temperature. Single-channel currents were amplified using an Axopatch-200B amplifier (Axon Instruments, Foster City, CA), filtered at 100 Hz, and computer transferred via an ITC-18 interface (Instrutech Corp., Port Washington, NY). Data were digitized at 2 kHz and written directly onto hard disk using Pulse 8.65 (HEKA, Lambrecht, Germany) software. The applied potential is the pipette electrode potential minus the bath electrode reference potential (+current: pipette to bath). Current records were analyzed by TAC software (Bruxton, Seattle, WA) and plotted using IgorPro (WaveMetrics, Lake Oswego, OR).

Results

Slc26a9 Expression and Chromosomal Localization

A 5-kb Slc26a9 transcript is found in lung and stomach of mouse and human (not shown). Both mouse Slc26a9 and human SLC26A9 have a predicted C-terminal type I PDZ interaction motif (SEV) (see Discussion).

Radiation hybrid mapping places human *SLC26A9* at chromosome 1q31-32. Murine *Slc26a9* is physically linked on Celera contigs to STS markers and genes (*cathepsin E*, *Mdm4*, *ELK4*, and *PCTK3)* located on the syntenic region of murine chromosome 1 at ~70 cM (Mouse Genome Database).

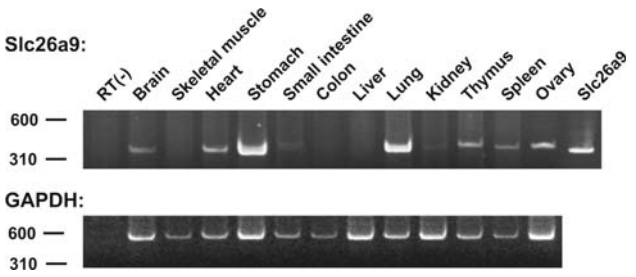

Fig. 1 Slc29a9 mRNA distribution. RT-PCR of mouse tissues showing the wider distribution of Slc26a9 mRNA (brain, heart, small intestine, kidney, thymus, spleen, and ovary)

RT-PCR showed that Slc26a9 is in lung and stomach and detectable in brain, heart, kidney, thymus, spleen, and ovary (Fig. 1).

Protein Localization

To determine Slc26a9 cellular localization, we generated a rabbit polyclonal, C-terminal-peptide antibody. The Slc26a9 antibody specificity was determined by assessing cross-reactivity with other recombinant Slc26 proteins expressed in oocytes (Fig. 2A). The Slc26a9 antibody recognizes a protein of ~87 kDa only from oocytes injected with Slc26a9 cRNA.

Next we examined the tissue Slc26a9 localization in mouse lung (Fig. 2B) and stomach (Fig. 2C and D). Staining is apparent in both bronchial epithelia and alveolar cells. The Slc26a9 blocking peptide (BP) eliminated lung staining (Fig. 2B, right).

Using an antibody to H^+/K^+-ATPase, we colocalized Slc26a9 with this marker of gastric crypt epithelia. Slc26a9 is found at the apical membrane of gastric surface epithelia and intracellular membranes (Fig. 2C and D) as reported by Xu et al. (2005). The Slc26a9 protein is also immunolocalized to apical membranes of gastric gland crypt epithelia (Fig. 2D). The stomach staining is eliminated by the Slc26a9-blocking peptide (Fig. 2C, right). Thus, Slc26a9 is highly expressed in both the less differentiated epithelial population (surface) and the terminally differentiated epithelia (crypt). Modest, yet obvious, Slc26a9 staining occurs in cells expressing the H^+/K^+-ATPase. Higher-magnification evaluation of these H^+/K^+-ATPase positive cells reveals some overlapping and some adjacent Slc26a9 staining (not shown).

HCO_3^- Transport

To determine if Slc26a9 functions as a Cl^--HCO_3^- exchanger, we measured intracellular pH (pH_i) changes

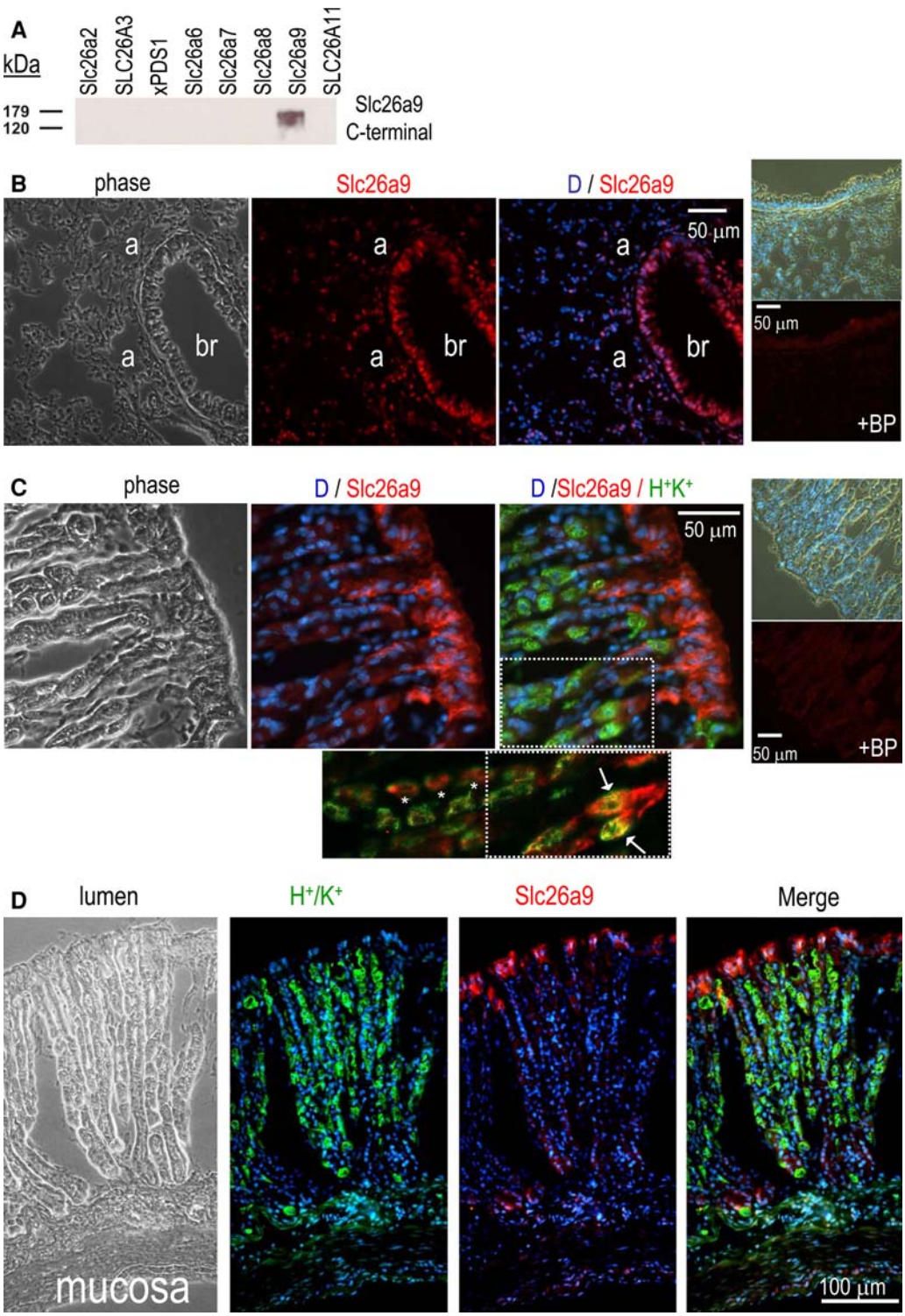

Fig. 2 Immunolocalization of Slc26a9 protein in lung and stomach. **A** Slc26 proteins were expressed in *Xenopus* oocytes by injecting cRNA. Rabbit polyclonal antibodies for Slc26a9 were used to probe Western blots of oocyte membranes. **B** Mouse lung tissue: Slc26a9 staining (cy3, red) with DAPI (blue, blue "D", nuclei). "a" designates alveoli and "br" designates bronchiole. Smaller right-hand panels show both phase and fluorescence of mouse lung in the presence of the Slc26a9 blocking peptide (BP). **C** Mouse stomach: colabeling of Slc26a9 (red), HK pump (green), and DAPI (blue; nuclei). Smaller right-hand panels show both phase and fluorescence of mouse stomach in the presence of the Slc26a9 BP. *Inset* Magnification and extension of the merged view. Removal of the DAPI stain and enhanced red contrast shows that there is both colocalization of Slc26a9 and the H^+/K^+ pump (arrows and yellow) and adjacent staining (*) in the central cells of the crypt. **D** A montage of the complete gastric crypt-villus axis: Slc26a9 (red), HK pump (green), DAPI (blue), and merge (red, green, blue fluorescent overlay)

after Cl^- removal and readdition from the CO_2/HCO_3^- bath solution. Since we and others have found that some Slc26 transporters are electrogenic (Ko et al. 2002; Xie et al. 2002a), we also measured V_m changes simultaneously. Water-injected oocytes exposed to bath CO_2/HCO_3^- acidified quickly (Fig. 3A and D). These and our previous results showed that Na^+- and Cl^--dependent HCO_3^- transport is absent from water-injected-oocytes (Romero et al. 1997, 2000; Xie et al. 2002a). The initial pH_i is similar for water control- and Slc26a9- or Slc26a7-expressed oocytes. Bath CO_2/HCO_3^- addition decreases the pH_i of Slc26a9-injected oocytes (Fig. 3B and E), similar to water control oocytes. HCO_3^- addition also causes a small depolarization in Slc26a9-injected oocytes (Fig. 3E), reminiscent of the anion conductance observed with NDAE1 (Romero et al. 2000) and Slc26a6 (Xie et al. 2002a). In water controls, Cl^- replacement (with gluconate; $0Cl^-$) did not change the pH_i or V_m. On the other hand, for Slc26a9, $0Cl^-$ increases the pH_i (alkalinization), which stops with Cl^- readdition. $0Cl^-$ also evokes a depolarization in Slc26a9-injected oocytes (Fig. 3E). By contrast, $0Cl^-$ hyperpolarized the Slc26a6 oocytes (Xie et al. 2002a). For Slc26a7-oocytes, $0Cl^-$ depolarized the oocyte but did not increase the pH_i (Fig. 3C) as observed with either Slc26a6 or Slc26a9. The rate of pH_i change (Fig. 3D) and V_m changes (Fig. 3E) associated with Cl^- removal were repeated for the second time after the readdition of Cl^-. For Slc26a9, $0Cl^-$ (in O_2 bubbled solutions; initial part of Fig. 3B) gave similar results ($\uparrow pH_i$, $+27 \pm 4.6 \times 10^{-5}$ pH units/s; ΔV_m, $+114 \pm 7.0$ mV; $n = 5$). Thus, Slc26a9 has a nCl^--OH^- exchange mode.

Acid-base transport via Slc26a9 is further evidenced by a pH_i overshoot. This overshoot is due to HCO_3^- loading of the oocyte due to prolonged exposure to CO_2/HCO_3^-. Prior to CO_2 removal, the pH_i rose to 7.1 (Fig. 3B). CO_2/HCO_3^- removal elicited a robust alkalinization and pH_i overshoot, to 7.7 (7.79 ± 0.11; $n = 7$), i.e., cell HCO_3^- loading ($+0.37 \pm 0.06$ pH unit > starting pH_i) (Romero et al. 1998, 2000). This overshoot is not observed in controls (Fig. 3A) or Slc26a7 oocytes (Fig. 3C). The Slc26a9 oocytes also showed a hyperpolarization ($\sim$5–7 mV) with CO_2/HCO_3^- removal.

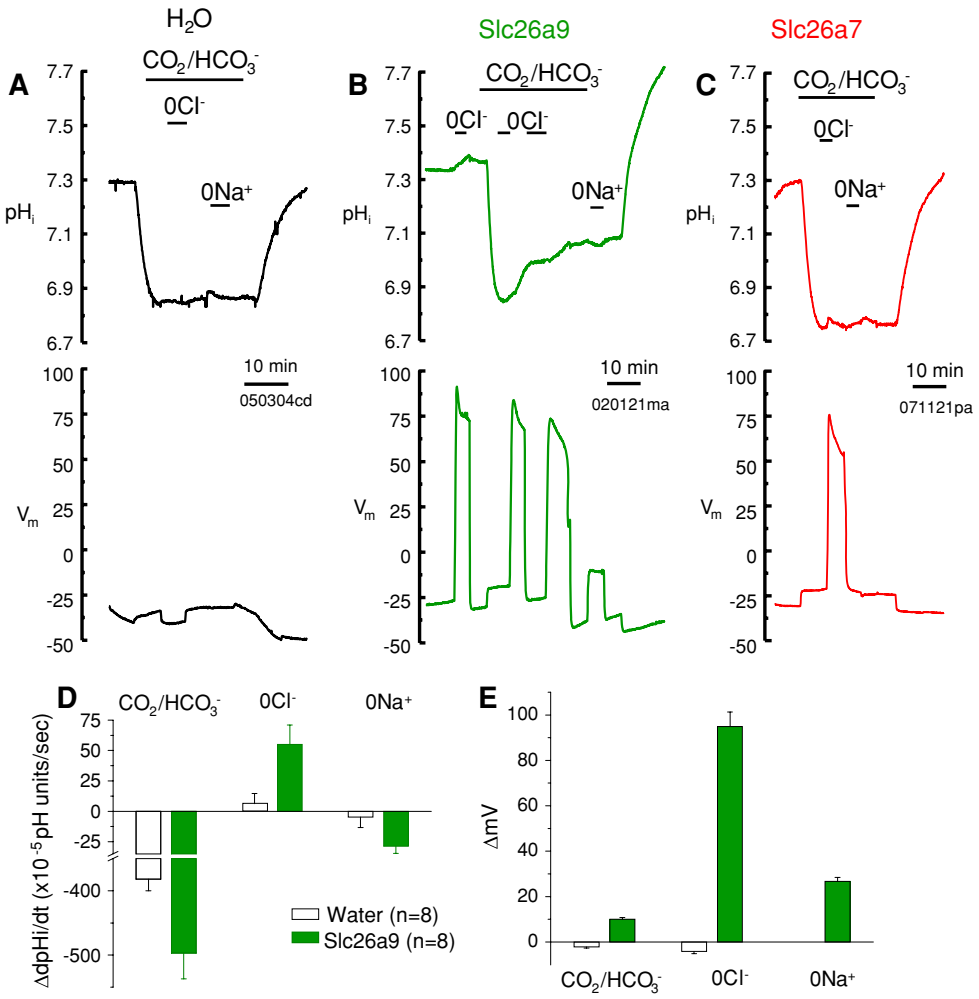

Fig. 3 Cl^--HCO_3^- exchange activity. Intracellular pH (pH_i) and membrane potential (V_m) changes of a water-injected *Xenopus* oocyte (**A**) and oocytes expressing Slc26a9 (**B**) or Slc26a7 (**C**) were measured using microelectrodes (see Methods). Bath Cl^- removal ($0Cl^-$; gluconate replacement) in the presence of 5% CO_2/33 mM HCO_3^- (pH 7.5) will increase the pH_i as Cl^- moves out of the oocyte in exchange for HCO_3^- (moving into the oocyte). Na^+ removal (in CO_2/HCO_3^-) is an indication of Na^+/HCO_3^- cotransporter activity (Na^+ and HCO_3^- moving out of the oocyte together). $0Cl^-$ elicits a pH_i increase (base loading) in Slc26a9 (**B**) cells but not Slc26a7 (**C**) cells. $0Cl^-$ also elicits a V_m increase for both Slc26a9 and Slc26a7. Averaged pHi change rates (10^{-5} pH unit/s; **D**) and membrane potential changes (ΔmV; **E**) due to addition of CO_2/HCO_3^-, Cl^- removal, and Na^+ removal. Text below time bar indicates the lab experimental number

Other than a dependence on bath pH, no Slc26 proteins have been shown to participate in cation transport. To test a potential role of Na^+ in Slc26a9-mediated transport, we replaced Na^+ with NMDG in CO_2/HCO_3^- solutions. Sodium removal depolarizes Slc26a9 oocytes (Fig. 3E) and the pH_i is also reduced (Fig. 3B; dpH_i/dt in Fig. 3D). This depolarization and acidification is similar to a "low-activity" electrogenic $Na^+/nHCO_3^-$ cotransporter (Romero et al. 1997), an activity not observed in control oocytes (Fig. 3A; dpH_i/dt in Fig. 3D; ΔV_m in Fig. 3E).

Cl^- Transport

The large depolarization resulting from $0Cl^-$ (HCO_3^- solution) implied that multiple intracellular Cl^- ions are exchanged for each extracellular HCO_3^- ($\underline{n}Cl^-$:$1HCO_3^-$). To directly examine Cl^- transport by Slc26a9, we measured intracellular Cl^- concentration ($[Cl^-]_i$) and V_m simultaneously (Fig. 4). Resting $[Cl^-]_i$ in Slc26a9-expressing oocytes was lower than in water-injected control oocytes (29.3 ± 2.8 mM [$n = 21$] vs. 39.4 ± 2.7 mM [$n = 14$], respectively). Unlike the control oocyte (Fig. 4A), Cl^- removal causes a vigorous $[Cl^-]_i$ decrease (Cl^- efflux) in the Slc26a9 oocyte (Fig. 4B). $0Cl^-$ elicited a rapid Cl^- drop (−5.1 mM Cl^-/min) such that in 5 min $[Cl^-]_i$ had fallen by 12–19 mM with a 60-mV depolarization. This dramatic $[Cl^-]_i$ fall was not observed in control oocytes (−0.62 mM Cl^-/min; Fig. 4A). Bath Cl^- readdition neither increased nor returned $[Cl^-]_i$ to initial levels (Fig. 4B), indicating that Cl^- efflux is Slc26a9's dominant mode.

Na^+ Transport

Based on our pH_i experimental results (Fig. 3A and B), we sought to determine if Na^+ altered Slc26a9-mediated transport. Specifically, does Slc26a9 transport Na^+?

Using Na^+ selective microelectrodes and ^{22}Na, we measured intracellular $[Na^+]$ ($[Na^+]_i$) changes and Na uptake in Slc26a9- and water-injected oocytes (Fig. 5). Resting $[Na^+]_i$ was similar in both water controls (Fig. 5A) and Slc26a9-expressing oocytes (Fig. 5B). $0Na^+$ caused a $[Na^+]_i$ decrease (Na^+ efflux, −0.48 ± 0.16 mM; $n = 8$) and a depolarization (+6.8 ± 0.7 mV; $n = 8$) in Slc26a9 oocytes (electrogenic $Na^+/\underline{n}$Anion cotransport) but not in controls (−6.6 ± 1.1 mV; $n = 7$). Simultaneous Cl^- removal ($0Na^+$-$0Cl^-$) resulted in a further $[Na^+]_i$ decrease (Fig. 5B) (−0.71 ± 0.23 mM; $n = 8$) and robust depolarization (>60 mV). Na^+ readdition raised the $[Na^+]_i$ in Slc26a9 oocytes (+1.31 ± 0.24 mM; $n = 8$), and sequential Cl^- readdition further increased $[Na^+]_i$ (+1.23 ± 0.18 mM; $n = 8$). $0Cl^-$ alone reversibly decreased $[Na^+]_i$ in Slc26a9 but not in control oocytes. Figure 5C shows that Slc26a9 oocytes, but not Slc26a6 oocytes, have a higher ^{22}Na uptake than water-injected control oocytes. This Na^+ transport is reversible, indicating that Slc26a9 participates in both Na^+ efflux (measured by electrodes) and Na^+ influx (measured by both electrodes and ^{22}Na). The conclusion on Na^+ transport by Slc26a9 is further strengthened by the result in Fig. 5D, showing that $^{36}Cl^-$ uptake by Slc26a9 was increased by the presence of extracellular Na^+ (500 pmol/oocyte/h).

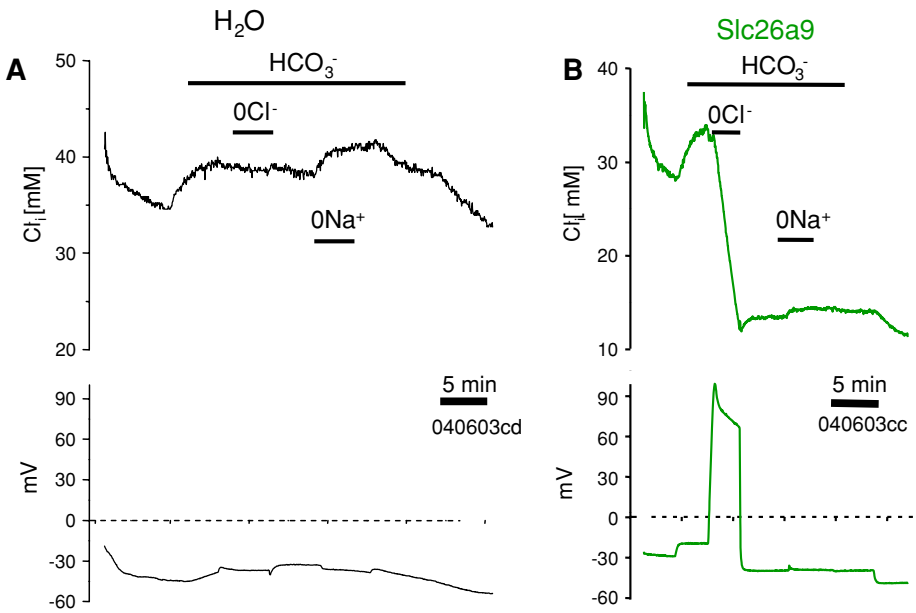

Fig. 4 Cl^- transport. Oocytes were perfused while monitoring $[Cl^-]_i$ (upper panels) and V_m (lower panels) for water (**A**) and Slc26a9 (**B**). Cl^- was replaced with gluconate and Na^+ was replaced with NMDG. Removal of Cl^- from the extracellular 33 mM HCO_3^- solution resulting in a dramatic fall in $[Cl^-]i$ and simultaneously depolarizing the cell depicts multiple Cl^- exchange for one HCO_3^- transport of Slc26a9

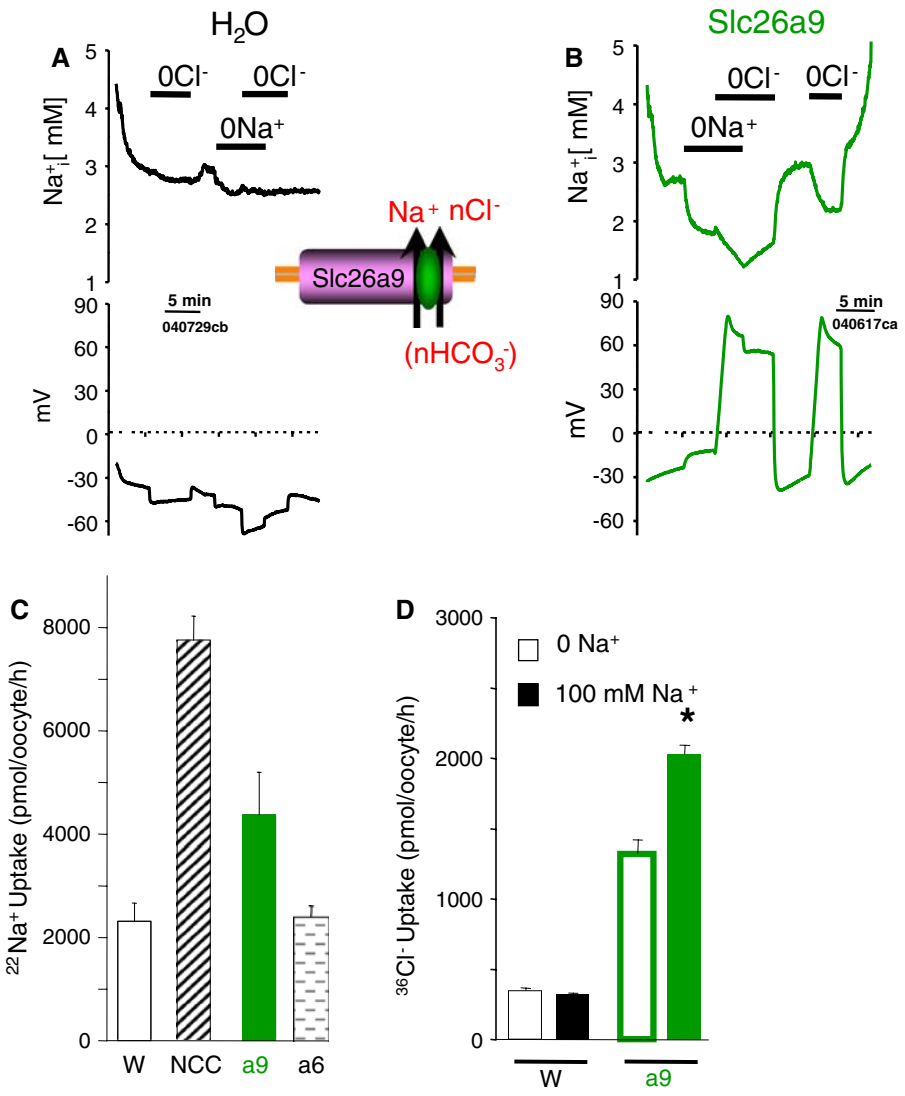

Fig. 5 Na^+ transport. Oocytes were perfused while monitoring $[Na^+]_i$ (upper panels) and V_m (lower panels) for water (**A**), and Slc26a9 (**B**). Cl^- was replaced with gluconate and Na^+ was replaced with NMDG. Removal of Na^+ from extracellular solution resulted in a slight depolarization of the cell in addition to a moderate decrease in $[Na^+]_i$ in Slc26a9. These two reversible transport modes are not observed in H_2O-injected oocytes under the same solution maneuver. **C** Robust and moderate $^{22}Na^+$ uptake were observed in the Na^+-Cl^- cotransporter (NCC, stripes) Slc26a9 (green), respectively, but not in Slc26a6 (speckled). These data again strengthened our hypothesis that Slc26a9 can transport Na^+ directly. **D** Slc26a9-mediated $^{36}Cl^-$ uptake is augmented by the presence of Na^+ in the uptake medium. Model after panel **A** indicates the likely modes of Na^+ transport by Slc26a9

Current-Voltage (I-V) Relationships

We previously reported large currents with Slc26a9 activity (Romero et al. 2006). Another report found similar activity (Dorwart et al. 2007) and examined the halide selectivity of human SLC26A9. With 25 ng of Slc26a9 cRNA, we could easily measure the "transporter" modes of Slc26a9. However, this amount of cRNA resulted in currents beyond the capabilities of our voltage clamp. Thus for voltage clamp experiments, we used injections of 0.5 ng/oocyte.

We tested the Cl^- and cation dependence of these currents (Slc26a9, Fig. 6A–C; control, Fig. 6D–F). In $0Cl^-$, oocyte currents are modest (Fig. 6A) but still higher than controls. Cl^- addition greatly increased Slc26a9 currents (>20 μA; Fig. 6B). Microelectrode experiments measuring a huge intracellular $[Cl^-]$ drop after Cl^- removal (Fig. 4B) also implicated Cl^- as the current charge carrier. Sodium removal ($0Na^+$) decreased the current magnitude, which again suggested that the Na^+-coupling of Slc26a9 transport $0Na^+$ minimized a time-dependent current (after 10 ms) but not the initial step currents (Fig. 6C). None of these Slc26a9-currents were observed in the water-control oocytes (Fig. 6D–F).

Anion Conductance

To determine if the large currents found in Slc26a9 were a "pure" Cl^- conductance (e.g., Cl^- channel), we varied the extracellular $[Cl^-]$ ($[Cl^-]_o$) while measuring $[Cl^-]_i$ and V_m (Fig. 7A). These experiments allowed us to compare the $[Cl^-]_i$ change in response to $[Cl^-]_o$ changes. There is a linear relationship between the equilibrium potential (E_{Cl}) and $[Cl^-]_o$ (15-104 mM). We also obtained I–V curves while varying bath Cl^- (Fig. 7B, left). These data show that the $I_{max}^{Cl^-}$ occurs when $[Cl^-]$ is >104 mM (Fig. 7B,

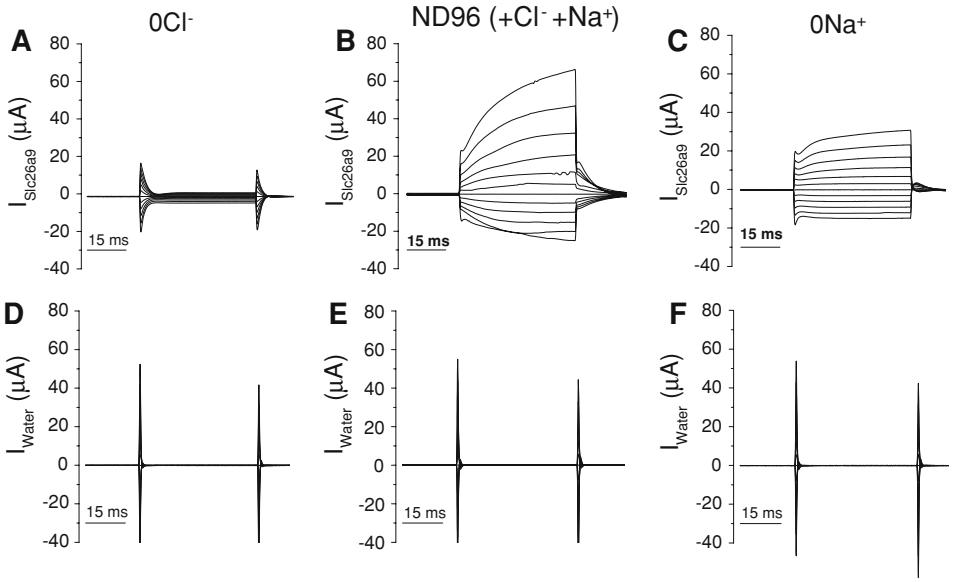

Fig. 6 Whole-cell currents of Slc26a9. Slc26a9-injected (**A**–**C**) and water-injected control (**D**–**F**) oocytes were voltage-clamped at −60 mV, and in various extracellular solutions, 40 ms I–V protocols were executed from a V_h of −160 mV to a V_h of +60 mV in 20-mV steps, then filtered at 2–5 kHz and recorded at 10 Hz. ND96 (**B**) has an extracellular Cl^- concentration of 104 mM and 96 mM Na^+. Cl^- was replaced with gluconate and Na^+ was replaced with NMDG

right). Next, we tested for asymmetric "channel gating," i.e., Can Slc26a9 Cl^- currents be activated or inactivated with a voltage pre-pulse (Fig. 7C: +60 mV, blue; resting V_m, black; −140 mV, red). These experiments illustrate that the Slc26a9 I–V relationships are not prepulse dependent and that there is no "inactivation" state as predicted in many channel kinetic schemes.

Patch Recordings

One-half-nanogram injections of Slc26a9 cRNA led to currents of tens of microamperes (Fig. 6), and Slc26a9 oocytes act as an almost-perfect Cl^- electrode (Fig. 7A). Therefore, we used inside-out excised patch-clamp experiments to determine if Slc26a9 expression (oocytes, HEK cells, and CHO cells) resulted in single-channel events (Fig. 8).

Figure 8A shows obvious single-channel events from one such patch (CHO cells). In symmetric NaCl solutions, holding at −100 mV resulted in a ~3.2-pS channel conductance. The Slc26a9 channel response to different holding potentials is shown in Fig. 8B. Similar channel activity was evident in oocytes and HEK cells (not shown). These single-channel events were not observed in non-transfected CHO control cells (Fig. 8C).

Discussion

The Slc26 protein family encodes diverse anion transporters which, when mutated, cause a variety of human diseases: diarrhea, deafness, goiter, diastrophic dysplasia, etc. Within this novel anion transporter group, the Slc26a9 protein displays further surprising functions, e.g., $n Cl^-$-HCO_3^- exchange, single Cl^- channels, and Na^+-coupling. Comparative genomic analysis indicates that the Slc26a9 gene may have arisen as recently as the emergence of amphibians but at least after teleosts (Romero, personal observation; see below).

Slc26a9 (electrogenic $n Cl^-$-HCO_3^- exchanger and Cl^- channel) branches with Slc26a5 (prestin, anion receptor) and Slc26a6 (electrogenic Cl^--$n HCO_3^-$ exchanger) in the Slc26 family. Yet Slc26a7 (apparent Cl^- channel conductance) is found in a different branch of the Slc26 family. "How" these disparate transport functions arose will require more detailed knowledge of the molecular determinants of anion recognition and transport.

Our uptake data for mouse Slc26a9 differ from those published for human SLC26A9 (Lohi et al. 2002). Lohi et al. (2002) reported that SLC26A9-injected cells mediate uptake of SO_4^{2-}, Cl^-, oxalate (ox^{2-}), and formate. Perhaps some differences are due to species variation, although mouse and human Slc26a9 are ~90% identical. Notably, the reported cis-inhibition data lack a positive control (e.g., Slc26a6) for the substrates tested. These cis-inhibition data also disagree with uptake measurements in the same study (Lohi et al. 2002), i.e., oxalate was a substrate but did not cis-inhibit $^{35}SO_4^{2-}$ uptake.

Similar discrepancies exist in the reported transport characteristics of other Slc26 paralogues. Several groups have reported that SLC26A3 transports SO_4^{2-}. Our data (Romero et al. 2006) and those of Chernova et al. (2003) indicate that SO_4^{2-} is not a human SLC26A3 substrate. Of note, we (Romero et al. 2006) and Chernova et al. (2003) found $^{36}Cl^-$ uptakes for Slc26a3 of 20- to 40-fold greater than for water controls, versus Moseley and coworkers'

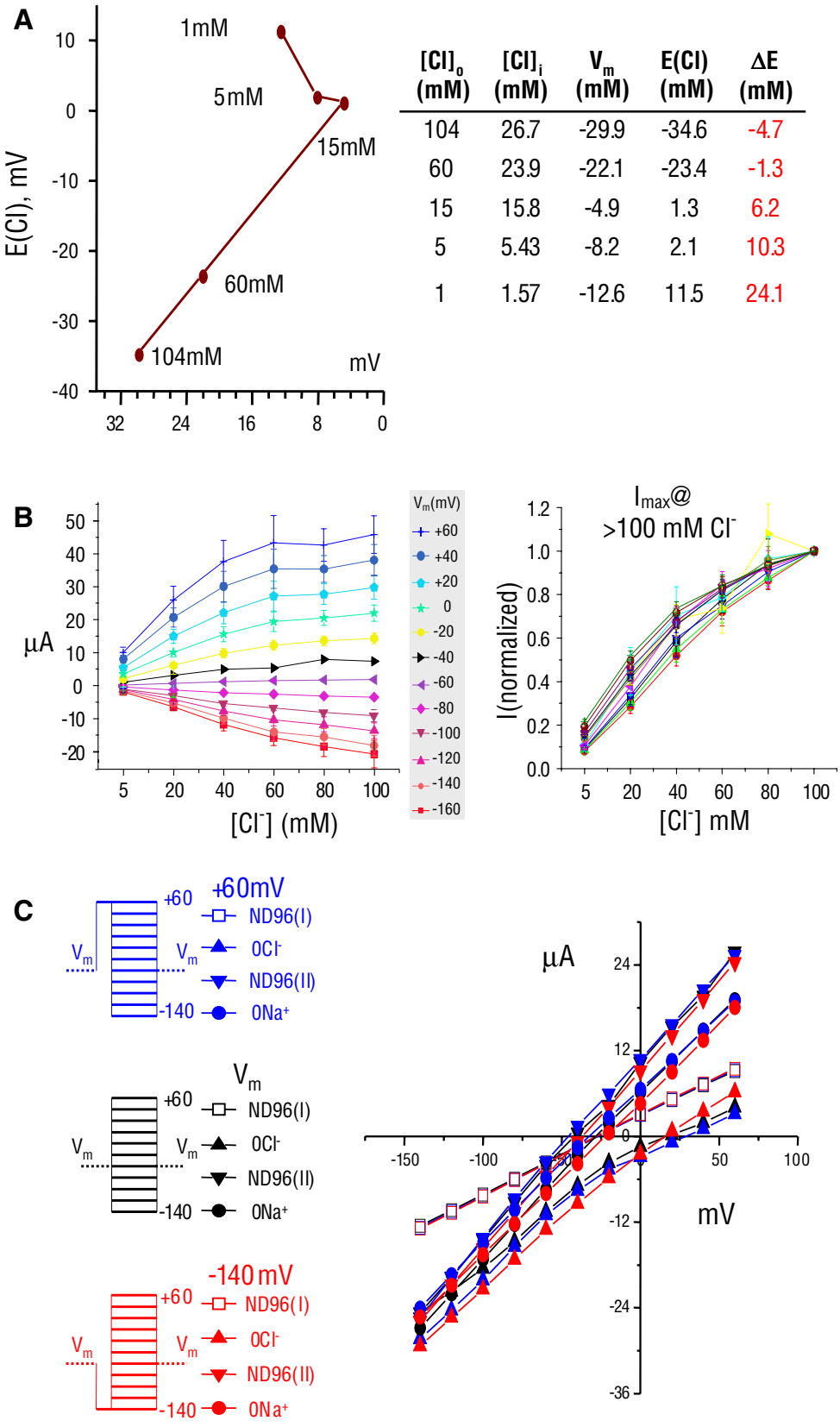

Fig. 7 Anion conductance of Slc26a9. **A** Intracellular Cl^- concentration $[Cl^-]_i$ and V_m were measured simultaneously, while the extracellular Cl^- concentrations ($[Cl^-]_o$) were varied from 1 to 104 mM. There is a linear relationship between the equilibrium potential (E[Cl]) and $[Cl^-]_o$ from 15 to 104 mM Cl^-. **B** Voltage clamp steps of Slc26a9 currents elicited by various extracellular Cl^- concentrations from 0 to 104 mM (left). Data shown are averaged values from 6 oocytes and color-coded for each holding voltage. Currents are normalized to values measured at 104 mM extracellular Cl^- at each respective holding voltage (right). These data also indicate that that the I(max) for Cl^- occurs at >104 mM. **C** Comparison of the I–V relationships for Slc26a9 at +60 mV (blue), resting V_m (black), or −140 mV (red) prepulse before the pulse protocol was executed while extracellular Cl^- or Na^+ were present (open squares, ND96[I]; filled inverted triangles, ND96[II]) or replaced (0Cl^-, filled triangles; 0Na^+, filled circles). The I–V relationships for Slc26a9 are not prepulse dependent

(1999) 1-fold greater than controls, the first report of SLC26A3 SO_4^{2-} transport. Consistent with Scott and Karniski's data, SLC26A4, the closest human SLC26A3 paralogue, is specific for monovalent anions and does not transport SO_4^{2-} (Scott and Karniski 2000; Scott et al. 1999).

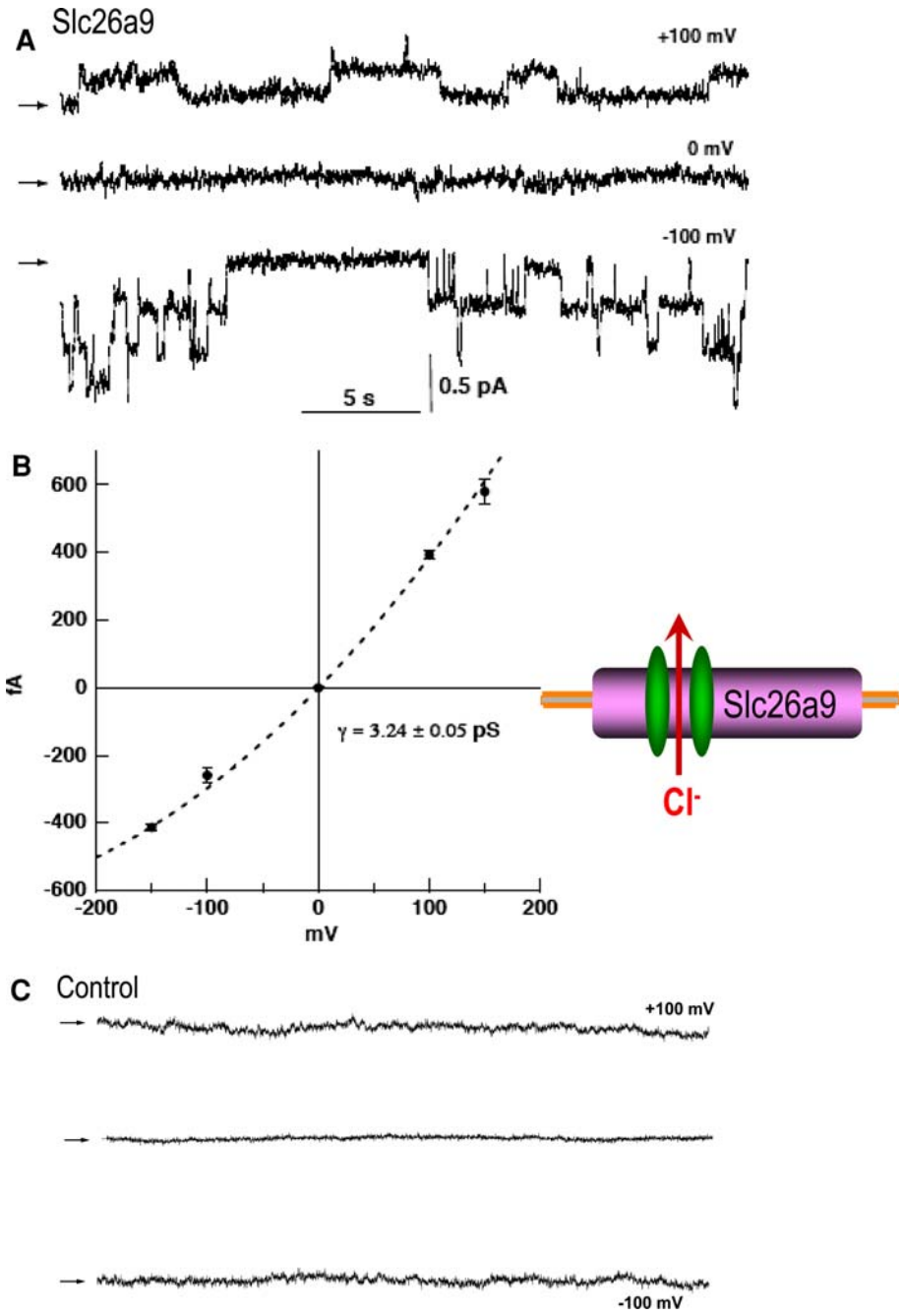

Fig. 8 Slc26a9 displays single-channel events. **A** Slc26a9 Cl^- channels in an inside-out patch with symmetrical (140 mM) NMDG-chloride at various pipette potentials (+100, 0, and −100 mV). Representative recordings are from CHO cells transiently expressing Slc26a9. Arrows indicate the baseline levels. **B** Single-channel current-voltage relationships of Slc26a9 channels. Data points are mean ± SE of three to six experiments at each voltage. The dotted line is the mean slope conductance fitted to the data points. **C** Recordings of nontransfected CHO cells at various pipette potentials (+100, 0, and −100 mV)

As with Slc26a6 (Xie et al. 2002a), we determined whether Slc26a9 was capable of Cl^--HCO_3^- exchange and what the nature of this exchange might be. ΔpH_i measurements elicited by the extracellular $0Cl^-$ ($+HCO_3^-$) showed that Slc26a9 functions as a nCl^--HCO_3^- exchanger (Fig. 3B). This same type of experiment showed that Slc26a6 was an electrogenic Cl^--$nHCO_3^-$ exchanger (Xie et al. 2002a). Slc26a7 (in an oocyte expression vector) had no obvious Cl^--HCO_3^- exchange (see Fig. 3C) as suggested previously (Petrovic et al. 2003). Collectively, these Slc26 transporters (a3, a4, a6, a9) represent novel physiological activities—electrogenic Cl^--HCO_3^- exchange—not anticipated by prior animal or tissue physiology studies (Ko et al. 2002; Xie et al. 2002a).

Our Slc26a9 characterization adds to the novel activities mediated by these Slc26 proteins. Cl^- removal evokes a significant depolarization and pH_i increase (HCO_3^- uptake). These Slc26a9 results differ from Slc26a6-injected oocyte data for which $0Cl^-$ causes a strong *hyperpolarization* (Kato et al. 2008; Ko et al. 2002; Kurita et al. 2008; Shcheynikov et al. 2006; Xie et al. 2002a). The data presented here are, however, consistent with either cation-

coupled HCO_3^- exchange for Cl^- (Na^+ driven Cl^--HCO_3^- exchange) or exchange of $n$$Cl^-$ for 1 HCO_3^- (electrogenic $n$$Cl^-$-$HCO_3^-$).

Slc26a9 is the first Slc26 member with cation-coupling. Specifically, Na^+ replacement by choline decreases pH_i and depolarizes Slc26a9-expressing oocytes (Fig. 3B) or reduces whole-cell currents (Fig. 6C). This novel aspect of Slc26a9 transport is similar to that of NBCe1 (Romero et al. 1998), i.e., electrogenic Na^+-coupled $n$$HCO_3^-$ cotransport. While there is both Na^+ and Cl^- dependence of transport, these modes do not appear to be interconnected with HCO_3^-. That is, Slc26a9 does not appear to be a different variety of Na^+-driven Cl^--HCO_3^- exchanger (Grichtchenko et al. 2001; Romero et al. 2000). Rather Slc26a9 apparently has two, noninterdependent transporter modes illustrated by (a) $[Na^+]_i$ changing with bath Cl^- removal (Fig. 5) yet (b) $[Cl^-]_i$ not changing with bath Na^+ removal (Fig. 4). In our hands, Slc26a9 is unique in showing activation of Cl^- uptake at extracellular pH 6 (Romero et al. 2006). We hypothesize that the "pH dependence" observed with other Slc26 proteins (Xie et al. 2002a) may be modified to be a transport site in Slc26a9, as Slc26a9 is likely the most recent addition to the *Slc26* genes.

Several lines of evidence indicate that the presence of cations influences Slc26a9-mediated transport. First, most of the Cl^- uptake experiments were performed under nominally Na^+-free conditions. When extracellular Na^+ is added to the uptake solution, Cl^- uptake by Slc26a9 is enhanced (Fig. 5D). Second, there is a large Na^+ dependent conductance of Slc26a9 that is also time dependent (Fig. 6). Third, Slc26a9 activity is increased by lowering the extracellular pH as we reported previously (Romero et al. 2006). This extracellular pH dependence is a 25-fold $[H^+]$ increase ($\sim$0.04–1.00 μM). Thus, this concentration change is a significant "cation-coupling" mode of Slc26a9. Forth, Xu et al. (2005) found that Slc26a9-mediated Cl^--HCO_3^- exchange was suppressed by NH_4^+. Since NH_4^+ is often a K^+ surrogate, it is unlikely to act as an interfering cation of the Slc26a9 transporter channel. Instead, the V_m change typically associated with high $[NH_4^+]$ (or high $[K^+]$) likely alters the Slc26a9-Cl^--HCO_3^- exchange activity since Slc26a9 is controlled by both concentration and electrical driving forces. Together, these data demonstrate a clear cation-coupling mode of Slc26a9.

Slc26a9 expression is highest in lung and stomach (Fig. 1). These epithelial cells have prominent CFTR expression and seem to play a major role in pulmonary fluid, Cl^-, and HCO_3^- excretion (Ballard et al. 1999). Several reports indicate Cl^--HCO_3^- exchange regulation by CFTR (Choi et al. 2001; Greeley et al. 2001; Wheat et al. 2000). CFTR can also alter the function of Slc26a3, -a4, and -a6 (Ko et al. 2004). Transfecting CFT-1 tracheal epithelial cells (homozygous Δ508-CFTR) with wild-type CFTR results in stimulation of Cl^--HCO_3^- exchange and SLC26A3 mRNA induction (Wheat et al. 2000). There is a correlation among CFTR mutants, Cl^--HCO_3^- exchange, and CF phenotype. Pancreatic insufficiency mutants do not promote cAMP-dependent Cl^--HCO_3^- exchange, yet this regulation is preserved in pancreatic sufficiency mutants (Choi et al. 2001). This is of particular importance since Slc26a9 mediates $n$$Cl^-$-$HCO_3^-$ exchange (Fig. 3). Moreover, the Slc26a9 Na^+ coupling may provide a "fail-safe" for gastric epithelia in anion or HCO_3^- absorption (Fig. 9), i.e., anion absorption without H^+ absorption or HCO_3^- secretion. This hypothesis of Slc26a9's role in stomach epithelial physiology is further supported by a recent report of an Slc26a9 knockout mouse (Xu et al. 2008). Slc26a9 −/− mice have extensive stomach pathology and a defect in gastric acid secretion. Interestingly, the defect in parietal cell acid secretion implies that Slc26a9 function in H^+/K^+-pump-positive cells (lower Slc26a9 protein in Fig. 2C and D) is rate limiting for function. These data, in light of the Slc26a9 knockout mouse, also illustrate that Slc26a9 contributes to functional HCl secretion and that complete protein overlap is not necessary.

Ko and coworkers (2004) demonstrated a mutually, stimulatory interaction between the CFTR R-domain and the STAS domains of Slc26a3 and Slc26a6. A type I PDZ motif in Slc26a9 suggests that it may "collaborate" with CFTR and other transporters at apical membranes of pulmonary epithelia (Ahn et al. 2001; Wang et al. 2000) or other tissues where Slc26a9 is found (Fig. 1D). This would be consistent with our protein localization shown in Fig. 2. Again, this localization is supported by the loss of cells in the Slc26a9 −/−a mouse (Xu et al. 2008).

There is significant overlap in Slc26 mRNA expression in certain tissues (intestine and secretory epithelia), indicative of physiological redundancy. For example, SLC26A6 is coexpressed with SLC26A9 in Calu-3 cells (Mount and Romero, unpublished observations), suggesting that both play a role in pulmonary HCO_3^- secretion. SLC26A3 and SLC26A6 (Greeley et al. 2001; Lohi et al. 2000) and SLC26A2 (Haila et al. 2001) are expressed apically in pancreatic ductal epithelia. SLC26A2 and SLC26A3 are coexpressed apically in colonic epithelia (Haila et al. 2001, 2000). This coexpression of SLC26 anion exchangers with overlapping transport functions likely has significant genetic and physiological consequences (Fig. 9). Key unresolved questions include the specific roles of individual paralogues in specific membranes of specific cell types, e.g., apical membranes of pulmonary epithelial cells, and the degree to which SLC26 paralogues are interdependent or dependent on CFTR transport and regulation.

The electrophysiology experiments here reveal that Slc26a9 has three major ion transport modes: electrogenic

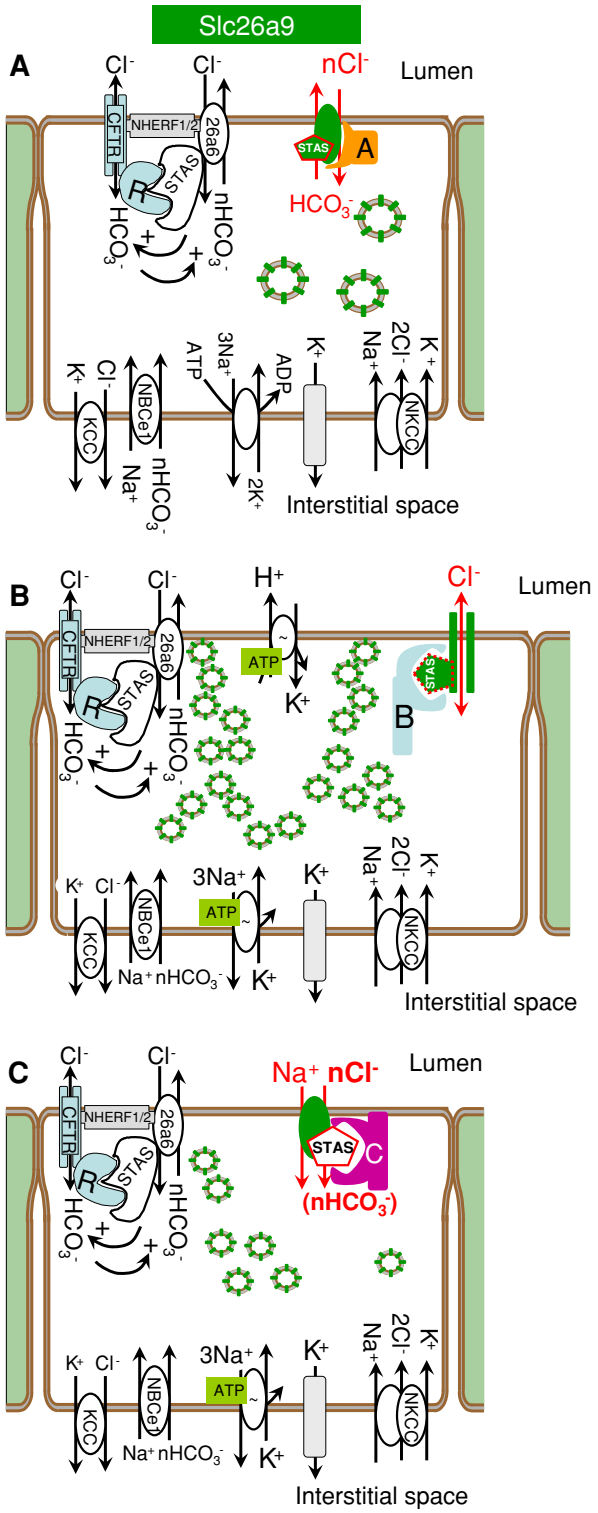

◀ **Fig. 9** Model of Slc26a9 function in stomach and lung. Epithelial cell models incorporating Slc26a9 at the apical membrane as a putative player in transepithelial NaCl absorption and H^+ secretion. **A** An epithelial cell which is both absorbing Cl^- and secreting HCO_3^-. Slc26a9 is also indicated in intracellular vesicles to be consistent with the intracellular staining observed. These putative vesicles could be recruited to the plasma membrane as a mechanism for controlling the amount of Slc26a9 plasma membrane function. **B** One potential model of H^+ in the gastric parietal cell (note extensive vesicles which would form the tubular canaliculi upon stimulation). While the parietal cell model shows Slc26a9 as a Cl^- channel, it is also possible to accomplish H^+ secretion with Slc26a9 as an electrogenic Cl^--HCO_3^- exchanger (**A**). **C** An epithelial cell in which Slc26a9 plays the role of a Na^+/*n*Anion$^-$ cotransporter. These panels also depict putative interacting proteins (**A**, **B** and **C**) that would "switch" the physiological mode of Slc26a9 (currently hypothetical)

nCl^--HCO_3^- exchange, electrogenic Na^+/*n*Anion$^-$ cotransport, and anion channel. Recently, the groups of Miller, Jentsch, and Pusch have provided compelling evidence that the distinction between channel and transporter is not as definitive as textbooks indicate (Accardi and Miller 2004; Picollo and Pusch 2005; Scheel et al. 2005). Likewise, our channel data (Fig. 8) and recent Slc26a9 cell conductance data (Dorwart et al. 2007) further blur the accepted distinctions of channels and transporters. Novel to Slc26a9 is that all three modalities are manifested by one protein, versus the functional separation in the CLC family, some paralogues having only Cl^-H^+ exchange and others displaying only channel activity.

The Slc26 gene family has a particular predilection for human genetic disease (Everett and Green 1999). The newer family members include positional and functional candidates for genetic disorders. SLC26A9 is a positional candidate for pseudohypoaldosteronism type II (Gordon's syndrome), an autosomal hypertensive disorder with linkage to chromosome 1 (Mansfield et al. 1997). Renal expression of SLC26A9 is not observed on Northern blots. However, Slc26a9 can be amplified by RT-PCR from mouse (Fig. 1D) and human kidney RNA (not shown), suggesting a role in renal NaCl absorption. SLC26A9 also seems to be regulated by the WNK1 and WNK4 kinases (Dorwart et al. 2007), the two known genes for pseudohypoaldosteronism type II.

Slc26a9 seems to be a recent addition to the *Slc26* genes, arising at least in amphibians since the *Slc26a9* gene is not found in teleosts such as zebrafish and fugu (Romero, personal observations). *Slc26a9* seems to be coincident with the emergence of "air-breathing." Species which are intermediate to amphibians and teleosts (boney fish, Class *Actinopterygii*), such as lung-fish (*Dipnoi*, which includes coelacanths), use a modified swim bladder or intestine to absorb O_2 (Bourbon and Chailley-Heu 2001; DeLaney et al. 1983). This connection may have led to Slc26a9 mRNA/protein expression in *Tetrapoda* being highest in lung and stomach. In the mudskipper (genus *Periophthalmus*) and weatherloach (*Misgurnus anguillicaudatus*), the transition from water extraction of O_2 to air-breathing arises manifesting as intestinal extraction of O_2 from air and thereby allowing estivation (Ip et al. 2004). Given the prominence of Slc26a9 mRNA in both lung and stomach, this evolutionary connection may associate Slc26a9 with

development of air-breathing. Or perhaps the novel transport features of Slc26a9 in the stomach and lung are due to selective pressures of terrestrial life or air breathing.

In conclusion, Slc26a9 is a widely expressed Slc26 paralogue, particularly abundant in lung and stomach. Slc26a9 moves inorganic ions by three distinct modes: (a) electrogenic $n\mathrm{Cl}^-$-HCO_3^- exchange, (b) electrogenic Na^+/nAnion cotransport, and (c) anion channel. Since many epithelial tissues have traces of Slc26a9 mRNA, discerning Slc26a9 functional roles in these tissues will be important and challenging. Redundancy or overlap of Slc26 protein expression complicates the physiological and structural contributions of this versatile protein family. Since the Slc26a3 and Slc26a6 STAS domains interact with CFTR (Ko et al. 2004) and PDZ-binding sites on Slc26 proteins, specific structures and protein interactions play a major role for this family (Fig. 9). The dynamics of these structural interactions are presently unknown. It is unlikely that these three distinct modes of Slc26a9 transport (electrogenic $n\mathrm{Cl}^-$-HCO_3^- exchanger [Fig. 9A], Cl^- channel [Fig. 9B], and Na^+/$n\mathrm{Anion}^-$ cotransporter [Fig. 9C]) are simultaneously functioning or even ever functioning in a given cell type. Accordingly, it is attractive to speculate that kinases/phosphatases, binding proteins, and domain structures may dictate the Slc26a9 physiology in specific tissues, e.g., channel (Fig. 9B) vs. transporter (Fig. 9A and C). For example, given the deficit in parietal cell H^+ secretion in the Slc26a9 knockout mouse (Xu et al. 2008), we would expect that either the Cl^- channel mode (Fig. 9B) or the electrogenic $n\mathrm{Cl}^-$-HCO_3^- exchanger mode (Fig. 9A) of Slc26a9 is missing in these mice. In other tissues where Slc26a9 expression is more limited (e.g., the kidney), there may be a physiologic need for a dynamic "switching" between these physiological modes to accommodate blood or intracellular signaling. Understanding these diverse functions and their potential regulation will help elucidate the role of SLC26A9 (human) in cystic fibrosis, defects in gastric acid secretion, pseudohypoaldosteronism type II, and other epithelial transport pathologies.

Acknowledgments We thank N. Angle, G. Babcock, L. Song, Q. Xie, R. Welch, and M. Sanders for excellent technical support. We thank Dr. S. Muallem for the Slc26a7 cDNA. We also thank Drs. S. W. Jones and C. Objero-Paz for discussions and initial patch experiments. This work was supported by NIH Grants DK056218, DK060845, and EY017732 (M.F.R.); DK038226, DK070756, and DK57708 (D.B.M.); and F32-DK65482 (V·B.). Other funding includes an Advanced Career Development Award from the Veterans Administration (DBM); the Wadsworth Foundation & American Heart Association (AHA; C.R.S.); a postdoctoral fellowship from the AHA (M.-H·C. and K.Z.); and the Cystic Fibrosis Foundation (ROMERO-06GO and SINDIC-06F0).

References

Accardi A, Miller C (2004) Secondary active transport mediated by a prokaryotic homologue of ClC Cl^- channels. Nature 427:803–807

Ahn W, Kim KH, Lee JA, Kim JY, Choi JY, Moe OW, Milgram SL, Muallem S, Lee MG (2001) Regulatory interaction between the cystic fibrosis transmembrane conductance regulator and HCO_3^- salvage mechanisms in model systems and the mouse pancreatic duct. J Biol Chem 276:17236–17243

Ballard ST, Trout L, Bebok Z, Sorscher EJ, Crews A (1999) CFTR involvement in chloride, bicarbonate, and liquid secretion by airway submucosal glands. Am J Physiol 277:L694–L699

Bissig M, Hagenbuch B, Stieger B, Koller T, Meier PJ (1994) Functional expression cloning of the canalicular sulfate transport system of rat hepatocytes. J Biol Chem 269:3017–3021

Bourbon JR, Chailley-Heu B (2001) Surfactant proteins in the digestive tract, mesentery, and other organs: evolutionary significance. Comp Biochem Physiol A Mol Integr Physiol 129:151–161

Chernova MN, Jiang L, Shmukler BE, Schweinfest CW, Blanco P, Freedman SD, Stewart AK, Alper SL (2003) Acute regulation of the SLC26A3 congenital chloride diarrhoea anion exchanger (DRA) expressed in *Xenopus* oocytes. J Physiol 549:3–19

Choi JY, Muallem D, Kiselyov K, Lee MG, Thomas PJ, Muallem S (2001) Aberrant CFTR-dependent HCO-3 transport in mutations associated with cystic fibrosis. Nature 410:94–97

DeLaney RG, Laurent P, Galante R, Pack AI, Fishman AP (1983) Pulmonary mechanoreceptors in the dipnoi lungfish *Protopterus* and *Lepidosiren*. Am J Physiol 244:R418–R428

Dinour D, Chang M-H, Satoh J-I, Smith BL, Angle N, Knecht A, Serban I, Holtzman EJ, Romero MF (2004) A novel missense mutation in the sodium bicarbonate cotransporter (NBCe1/SLC4A4) causes proximal tubular acidosis and glaucoma through ion transport defects. J Biol Chem 279:52238–52246

Dorwart MR, Shcheynikov N, Wang Y, Stippec S, Muallem S (2007) SLC26A9 is a Cl channel regulated by the WNK kinases. J Physiol 584:333–345

Everett LA, Green ED (1999) A family of mammalian anion transporters and their involvement in human genetic diseases. Hum Mol Genet 8:1883–1891

Everett LA, Glaser B, Beck JC, Idol JR, Buchs A, Heyman M, Adawi F, Hazani E, Nassir E, Baxevanis AD, Sheffield VC, Green ED (1997) Pendred syndrome is caused by mutations in a putative sulphate transporter gene (PDS). Nat Genet 17:411–422

Greeley T, Shumaker H, Wang Z, Schweinfest CW, Soleimani M (2001) Downregulated in adenoma and putative anion transporter are regulated by CFTR in cultured pancreatic duct cells. Am J Physiol Gastrointest Liver Physiol 281:G1301–G1308

Grichtchenko II II, Choi II, Zhong X, Bray-Ward P, Russell JM, Boron WF (2001) Cloning, characterization and chromosomal mapping of a human electroneutral Na+-driven Cl-HCO_3 exchanger. J Biol Chem 276:8358–8363

Haila S, Saarialho-Kere U, Karjalainen-Lindsberg ML, Lohi H, Airola K, Holmberg C, Hastbacka J, Kere J, Hoglund P (2000) The congenital chloride diarrhea gene is expressed in seminal vesicle, sweat gland, inflammatory colon epithelium, and in some dysplastic colon cells. Histochem Cell Biol 113:279–286

Haila S, Hastbacka J, Bohling T, Karjalainen-Lindsberg ML, Kere J, Saarialho-Kere U (2001) Slc26a2 (diastrophic dysplasia sulfate transporter) is expressed in developing and mature cartilage but also in other tissues and cell types. J Histochem Cytochem 49:973–982

Hastbacka J, de la Chapelle A, Kaitila I, Sistonen P, Weaver A, Lander E (1992) Linkage disequilibrium mapping in isolated founder populations: diastrophic dysplasia in Finland. Nat Genet 2:204–211

Hastbacka J, Superti-Furga A, Wilcox WR, Rimoin DL, Cohn DH, Lander ES (1996) Sulfate transport in chondrodysplasia. Ann NY Acad Sci 785:131–136

Hoglund P, Haila S, Scherer SW, Tsui LC, Green ED, Weissenbach J, Holmberg C, de la Chapelle A, Kere J (1996) Positional candidate genes for congenital chloride diarrhea suggested by high-resolution physical mapping in chromosome region 7q31. Genome Res 6:202–210

Ip YK, Chew SF, Randall DJ (2004) Five tropical air-breathing fishes, six different strategies to defend against ammonia toxicity on land. Physiol Biochem Zool 77:768–782

Karniski LP, Lotscher M, Fucentese M, Hilfiker H, Biber J, Murer H (1998) Immunolocalization of sat-1 sulfate/oxalate/bicarbonate anion exchanger in the rat kidney. Am J Physiol 275:F79–F87

Kato A, Chang M-H, Kurita Y, Nakada T, Hirose S, Romero MF (2008) Functional characterization of pufferfish Slc26a6A and Slc26a6B. FASEB J 22:936

Kim KH, Shcheynikov N, Wang Y, Muallem S (2005) SLC26A7 Is a Cl^- Channel Regulated by Intracellular pH. J Biol Chem 280:6463–6470

Knauf F, Yang CL, Thomson RB, Mentone SA, Giebisch G, Aronson PS (2001) Identification of a chloride-formate exchanger expressed on the brush border membrane of renal proximal tubule cells. Proc Natl Acad Sci USA 98:9425–9430

Ko SB, Shcheynikov N, Choi JY, Luo X, Ishibashi K, Thomas PJ, Kim JY, Kim KH, Lee MG, Naruse S, Muallem S (2002) A molecular mechanism for aberrant CFTR-dependent HCO_3^- transport in cystic fibrosis. EMBO J 21:5662–5672

Ko SB, Zeng W, Dorwart MR, Luo X, Kim KH, Millen L, Goto H, Naruse S, Soyombo A, Thomas PJ, Muallem S (2004) Gating of CFTR by the STAS domain of SLC26 transporters. Nat Cell Biol 6:343–350

Kurita Y, Nakada T, Kato A, Mistry AC, Chang M-H, Romero MF, Hirose S (2008) Identification of intestinal bicarbonate transporters involved in formation of carbonate precipitates to stimulate water absorption in marine teleost fish. Am J Physiol Comp Reg Physiol 284:R1402–R1412

Liman ER, Tytgat J, Hess P (1992) Subunit stoichiometry of a mammalian K+ channel determined by construction of multimeric cDNAs. Neuron 9:861–871

Lohi H, Kujala M, Kerkela E, Saarialho-Kere U, Kestila M, Kere J (2000) Mapping of five new putative anion transporter genes in human and characterization of SLC26A6, a candidate gene for pancreatic anion exchanger. Genomics 70:102–112

Lohi H, Kujala M, Makela S, Lehtonen E, Kestila M, Saarialho-Kere U, Markovich D, Kere J (2002) Functional characterization of three novel tissue-specific anion exchangers SLC26A7, -A8, and -A9. J Biol Chem 277:14246–14254

Mansfield TA, Simon DB, Farfel Z, Bia M, Tucci JR, Lebel M, Gutkin M, Vialettes B, Christofilis MA, Kauppinen-Makelin R, Mayan H, Risch N, Lifton RP (1997) Multilocus linkage of familial hyperkalaemia and hypertension, pseudohypoaldosteronism type II, to chromosomes 1q31–42 & 17p11–q21. Nat Genet 16:202–205

Moseley RH, Hoglund P, Wu GD, Silberg DG, Haila S, de la Chapelle A, Holmberg C, Kere J (1999) Downregulated in adenoma gene encodes a chloride transporter defective in congenital chloride diarrhea. Am J Physiol 276:G185–G192

Mount DB, Romero MF (2004) The SLC26 gene family of multifunctional anion exchangers. Pflügers Arch 447:710–721

Mount DB, Baekgaard A, Hall AE, Plata C, Xu J, Beier DR, Gamba G, Hebert SC (1999) Isoforms of the Na-K-2Cl cotransporter in murine TAL I. Molecular characterization and intrarenal localization. Am J Physiol 276:F347–F358

Petrovic S, Ju X, Barone S, Seidler U, Alper SL, Lohi H, Kere J, Soleimani M (2003) Identification of a basolateral Cl^-/HCO_3^- exchanger specific to gastric parietal cells. Am J Physiol Gastrointest Liver Physiol 284:G1093–G1103

Picollo A, Pusch M (2005) Chloride/proton antiporter activity of mammalian CLC proteins ClC-4 and ClC-5. Nature 436:420–423

Plata C, Sussman CR, Sindic A, Liang JO, Mount DB, Josephs ZM, Chang M-H, Romero MF (2007) A novel electroneutral sodium monocarboxylate transport (SMCTn) is present in zebrafish: a comparison to the electrogenic SMCT (SMCTe/Slc5a8). J Biol Chem 282:11996–12009

Romero MF, Hediger MA, Boulpaep EL, Boron WF (1997) Expression cloning and characterization of a renal electrogenic Na^+/HCO_3^- cotransporter. Nature 387:409–413

Romero MF, Fong P, Berger UV, Hediger MA, Boron WF (1998) Cloning and functional expression of rNBC, an electrogenic Na^+-HCO_3^- cotransporter from rat kidney. Am J Physiol 274:F425–F432

Romero MF, Henry D, Nelson S, Harte PJ, Dillon AK, Sciortino CM (2000) Cloning and characterization of a Na^+ driven anion exchanger (NDAE1): a new bicarbonate transporter. J Biol Chem 275:24552–24559

Romero MF, Chang M-H, Plata C, Zandi-Nejad K, Broumand V, Sussman CR, Mount DB (2006) Physiology of electrogenic SLC26 paralogs. In: Epithelial anion transport in health and disease: the role of the SLC26 transporters family. Novartis Foundation Symposium 273:126–147

Satoh H, Susaki M, Shukunami C, Iyama K, Negoro T, Hiraki Y (1998) Functional analysis of diastrophic dysplasia sulfate transporter. Its involvement in growth regulation of chondrocytes mediated by sulfated proteoglycans. J Biol Chem 273:12307–12315

Scheel O, Zdebik AA, Lourdel S, Jentsch TJ (2005) Voltage-dependent electrogenic chloride/proton exchange by endosomal CLC proteins. Nature 436:424–427

Schmitt BM, Biemesderfer D, Boulpaep EL, Romero MF, Boron WF (1999) Immunolocalization of the electrogenic Na^+/HCO_3^- cotransporter in mammalian and amphibian kidney. Am J Physiol 276:F27–F36

Schweinfest CW, Henderson KW, Suster S, Kondoh N, Papas TS (1993) Identification of a colon mucosa gene that is down-regulated in colon adenomas and adenocarcinomas. Proc Natl Acad Sci USA 90:4166–4170

Sciortino CM, Romero MF (1999) Cation and voltage dependence of rat kidney, electrogenic Na^+/HCO_3^- cotransporter, rkNBC, expressed in oocytes. Am J Physiol 277:F611–F623

Sciortino CM, Fletcher BR, Shrode LD, Harte PJ, Romero MF (2001) Localization of endogenous and recombinant Na^+-driven anion exchanger protein, NDAE1, from *Drosophila melanogaster*. Am J Physiol Cell Physiol 281:C449–C463

Scott DA, Karniski LP (2000) Human pendrin expressed in *Xenopus laevis* oocytes mediates chloride/formate exchange. Am J Physiol Cell Physiol 278:C207–C211

Scott DA, Wang R, Kreman TM, Sheffield VC, Karniski LP (1999) The Pendred syndrome gene encodes a chloride-iodide transport protein. Nat Genet 21:440–443

Shcheynikov N, Wang Y, Park M, Ko SB, Dorwart M, Naruse S, Thomas PJ, Muallem S (2006) Coupling modes and stoichiometry of Cl-/HCO3- exchange by slc26a3 and slc26a6. J Gen Physiol 127:511–524

Soleimani M, Greeley T, Petrovic S, Wang Z, Amlal H, Kopp P, Burnham CE (2001) Pendrin: an apical $Cl^-/OH^-/HCO_3^-$ exchanger in the kidney cortex. Am J Physiol Renal Physiol 280:F356–F364

Wang S, Yue H, Derin RB, Guggino WB, Li M (2000) Accessory protein facilitated CFTR-CFTR interaction, a molecular mechanism to potentiate the chloride channel activity. Cell 103:169–179

Wheat VJ, Shumaker H, Burnham C, Shull GE, Yankaskas JR, Soleimani M (2000) CFTR induces the expression of DRA along with Cl(–)/HCO(3)(–) exchange activity in tracheal epithelial cells. Am J Physiol Cell Physiol 279:C62–C71

Xie Q, Welch R, Mercado A, Romero MF, Mount DB (2002a) Molecular and functional characterization of the Slc26A6 anion exchanger, functional comparison to Slc26a1. Am J Physiol Renal Physiol 283:F826–F838

Xie Q, Welch R, Song L, Romero MF, Mount DB (2002b) Cloning of multiple novel members of the SLC26 gene family of anion exchangers. FASEB J 16:a807

Xu J, Henriksnas J, Barone S, Witte D, Shull GE, Forte JG, Holm L, Soleimani M (2005) SLC26A9 is expressed in gastric surface epithelial cells, mediates Cl^-/HCO_3^- exchange and is inhibited by NH_4^+. Am J Physiol Cell Physiol 289:C493–C505

Xu J, Song P, Miller ML, Borgese F, Barone S, Riederer B, Wang Z, Alper SL, Forte JG, Shull GE, Ehrenfeld J, Seidler U, Soleimani M (2008) Deletion of the chloride transporter Slc26a9 causes loss of tubulovesicles in parietal cells and impairs acid secretion in the stomach. Proc Natl Acad Sci USA 105:17955–17960

Zheng J, Shen W, He DZ, Long KB, Madison LD, Dallos P (2000) Prestin is the motor protein of cochlear outer hair cells. Nature 405:149–155